Yoash Levron
The Andrew and Erna Viterbi Faculty of Electrical Engineering, Technion—Israel Institute of Technology, Haifa 3200003, Israel
yoashl@ee.technion.ac.il

Juri Belikov
Department of Software Science, Tallinn University of Technology, Akadeemia tee 15a, 12618 Tallinn, Estonia
juri.belikov@taltech.ee

Lecture 2: The Direct-Quadrature-Zero (DQ0) Transformation

In the previous lecture we discussed the concept of time-varying phasor models (quasi-static models). We have seen that such models map sinusoidal signals to constants, and thus considerably simply the analysis of AC power systems. Nevertheless, time-varying phasors are an approximation, and can only be used if variations in amplitudes and phases are relatively slow.

This lecture introduces the $dq0$ transformation, and shows how to use it to analyze linear networks. Similar to phasors, the $dq0$ transformation maps sinusoidal signals to constants, and therefore results in relatively simple dynamic models. However this mapping is accurate, and does not rely on any approximations. Therefore $dq0$ models may be viewed as a natural extension of time-varying phasor models, and are used extensively for modeling and analysis of fast transient phenomena in power systems.

Table 1: The relative advantages of different dynamic models

	equilibrium points	small-signal	fast transients	nonsymmetric networks
abc	X	X	✓	✓
time-varying phasors	✓	✓	X	X
$dq0$	✓	✓	✓	see text

Basic definitions

The $dq0$ transformation and its inverse are defined as follows:

$$T_\theta = \frac{2}{3}\begin{bmatrix} \cos(\theta) & \cos\left(\theta-\frac{2\pi}{3}\right) & \cos\left(\theta+\frac{2\pi}{3}\right) \\ -\sin(\theta) & -\sin\left(\theta-\frac{2\pi}{3}\right) & -\sin\left(\theta+\frac{2\pi}{3}\right) \\ \frac{1}{2} & \frac{1}{2} & \frac{1}{2} \end{bmatrix}, \tag{1}$$

$$T_\theta^{-1} = \begin{bmatrix} \cos(\theta) & -\sin(\theta) & 1 \\ \cos\left(\theta-\frac{2\pi}{3}\right) & -\sin\left(\theta-\frac{2\pi}{3}\right) & 1 \\ \cos\left(\theta+\frac{2\pi}{3}\right) & -\sin\left(\theta+\frac{2\pi}{3}\right) & 1 \end{bmatrix}, \tag{2}$$

where the angle θ is the *reference angle* or the *reference phase*. Direct multiplication of these matrices reveals that $T_\theta T_\theta^{-1} = T_\theta^{-1} T_\theta = I_{3\times 3}$. Note that several variations of (1) are available in the literature.

The $dq0$ transformation maps three-phase signals in the abc reference frame to new quantities in a rotating $dq0$ reference frame. Denote $x_{abc} = [x_a, x_b, x_c]^\mathsf{T}$ and $x_{dq0} = [x_d, x_q, x_0]^\mathsf{T}$, then

$$\begin{aligned} x_{dq0} &= T_\theta x_{abc}, \\ x_{abc} &= T_\theta^{-1} x_{dq0}, \end{aligned} \tag{3}$$

where the subscripts d, q, and 0 represent the *direct*, *quadrature* and *zero* components. The reference angle θ is typically selected as follows:

- ✓ If there is an infinite bus in the system a typical choice is $\theta = \omega_s t$, where ω_s is the frequency of the infinite bus.
- ✓ If there is no infinite bus in the system, θ is usually fixed to the rotor angle of one of the synchronous machines.

Different selections of the reference angle will be discussed in the following lectures.

A fundamental property of the $dq0$ transformation is that it maps balanced three-phase signals to constants. For instance, consider a three-phase voltage source modeled as

$$\begin{aligned} v_a &= A\cos(\omega_s t), \\ v_b &= A\cos\left(\omega_s t - \frac{2\pi}{3}\right), \\ v_c &= A\cos\left(\omega_s t + \frac{2\pi}{3}\right). \end{aligned} \tag{4}$$

Applying the inverse transformation T_θ^{-1} with $\theta = \omega_s t$ leads to

$$\begin{bmatrix} v_a \\ v_b \\ v_c \end{bmatrix} = \begin{bmatrix} \cos(\omega_s t) & -\sin(\omega_s t) & 1 \\ \cos\left(\omega_s t - \frac{2\pi}{3}\right) & -\sin\left(\omega_s t - \frac{2\pi}{3}\right) & 1 \\ \cos\left(\omega_s t + \frac{2\pi}{3}\right) & -\sin\left(\omega_s t + \frac{2\pi}{3}\right) & 1 \end{bmatrix} \begin{bmatrix} A \\ 0 \\ 0 \end{bmatrix}, \tag{5}$$

and therefore $v_d = A$, $v_q = 0$, $v_0 = 0$. The sinusoidal signals in the abc reference frame are mapped to constant signals in the $dq0$ reference frame (see Fig. 1).

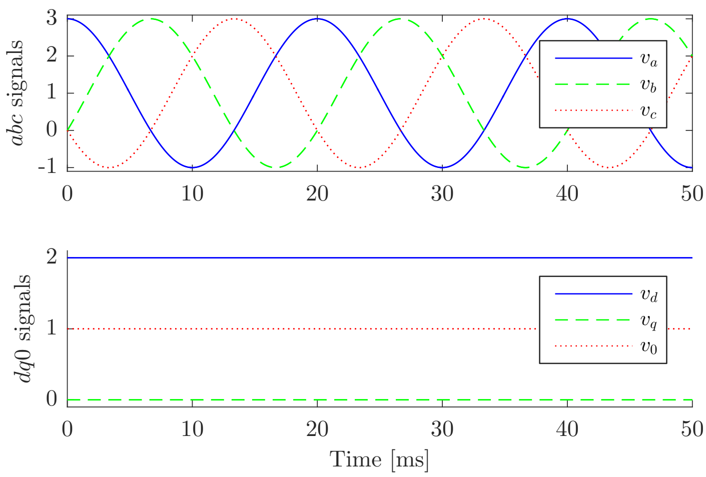

Figure 1: Mapping of sinusoidal abc signals to constant $dq0$ signals.

Modeling resistors, inductors, and capacitors

This section presents basic $dq0$ models of linear passive components. We will use the following definitions:

- ✓ *Balanced* three-phase signals are sinusoidal signals with equal magnitudes, phase shifts of $\pm 120°$, and a sum of zero.
- ✓ A power network is *balanced* or *symmetrically configured* if balanced three-phase voltages at its ports result in balanced three-phase currents, and vice-versa. Two examples are shown in Fig. 2.

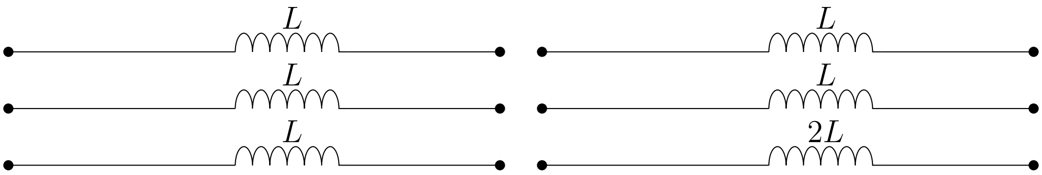

(a) Symmetrically configured network (b) Network with a non-symmetric configuration

Figure 2: Example of symmetric and nonsymmetric configurations.

In this text we will use the term *balanced* when referring to signals, and *symmetrically configured* when referring to three-phase networks or circuits.

Assume a symmetrically configured three-phase resistor R, which is modeled as

$$\begin{bmatrix} v_a \\ v_b \\ v_c \end{bmatrix} = R \begin{bmatrix} i_a \\ i_b \\ i_c \end{bmatrix} . \tag{6}$$

Multiplying both sides of the equation by the $dq0$ transformation T_θ (from the left) yields

$$\begin{bmatrix} v_d \\ v_q \\ v_0 \end{bmatrix} = R \begin{bmatrix} i_d \\ i_q \\ i_0 \end{bmatrix} . \tag{7}$$

This is the $dq0$ model of a symmetrically configured three-phase resistor.

Now assume a symmetrically configured three-phase inductor L, which is modeled as

$$\begin{bmatrix} v_a \\ v_b \\ v_c \end{bmatrix} = L \frac{\mathrm{d}}{\mathrm{d}t} \begin{bmatrix} i_a \\ i_b \\ i_c \end{bmatrix} . \tag{8}$$

The identity $[i_a, i_b, i_c]^\mathsf{T} = T_\theta^{-1} [i_d, i_q, i_0]^\mathsf{T}$ leads to

$$\begin{bmatrix} v_a \\ v_b \\ v_c \end{bmatrix} = L \frac{\mathrm{d}}{\mathrm{d}t} \left(T_\theta^{-1} \begin{bmatrix} i_d \\ i_q \\ i_0 \end{bmatrix} \right) , \tag{9}$$

and the derivative product rule yields

$$\begin{bmatrix} v_a \\ v_b \\ v_c \end{bmatrix} = L \left(\frac{\mathrm{d}}{\mathrm{d}t} T_\theta^{-1} \right) \begin{bmatrix} i_d \\ i_q \\ i_0 \end{bmatrix} + L T_\theta^{-1} \frac{\mathrm{d}}{\mathrm{d}t} \begin{bmatrix} i_d \\ i_q \\ i_0 \end{bmatrix} . \tag{10}$$

By direct computation it can be verified that

$$\frac{\mathrm{d}}{\mathrm{d}t}T_\theta^{-1} = -T_\theta^{-1}\mathcal{W} \tag{11}$$

with

$$\mathcal{W} = \begin{bmatrix} 0 & \frac{\mathrm{d}}{\mathrm{d}t}\theta & 0 \\ -\frac{\mathrm{d}}{\mathrm{d}t}\theta & 0 & 0 \\ 0 & 0 & 0 \end{bmatrix}. \tag{12}$$

Substituting these expressions in (10) yields

$$\begin{bmatrix} v_a \\ v_b \\ v_c \end{bmatrix} = -LT_\theta^{-1}\mathcal{W}\begin{bmatrix} i_d \\ i_q \\ i_0 \end{bmatrix} + LT_\theta^{-1}\frac{\mathrm{d}}{\mathrm{d}t}\begin{bmatrix} i_d \\ i_q \\ i_0 \end{bmatrix}, \tag{13}$$

and by multiplying both sides of the equation from the left by T_θ we have

$$\begin{bmatrix} v_d \\ v_q \\ v_0 \end{bmatrix} = -L\mathcal{W}\begin{bmatrix} i_d \\ i_q \\ i_0 \end{bmatrix} + L\frac{\mathrm{d}}{\mathrm{d}t}\begin{bmatrix} i_d \\ i_q \\ i_0 \end{bmatrix}, \tag{14}$$

which is equivalent to

$$\frac{\mathrm{d}}{\mathrm{d}t}\begin{bmatrix} i_d \\ i_q \\ i_0 \end{bmatrix} = \mathcal{W}\begin{bmatrix} i_d \\ i_q \\ i_0 \end{bmatrix} + \frac{1}{L}\begin{bmatrix} v_d \\ v_q \\ v_0 \end{bmatrix}. \tag{15}$$

This is the $dq0$ model of a symmetrically configured inductor. The explicit expressions are

$$\begin{aligned} \frac{\mathrm{d}}{\mathrm{d}t}i_d &= \frac{\mathrm{d}\theta}{\mathrm{d}t}i_q + \frac{1}{L}v_d, \\ \frac{\mathrm{d}}{\mathrm{d}t}i_q &= -\frac{\mathrm{d}\theta}{\mathrm{d}t}i_d + \frac{1}{L}v_q, \\ \frac{\mathrm{d}}{\mathrm{d}t}i_0 &= \frac{1}{L}v_0. \end{aligned} \tag{16}$$

Note that i_d affects the dynamics of i_q and vice-versa. Similarly, the dynamic model of a symmetrically configured capacitor C is

$$\frac{\mathrm{d}}{\mathrm{d}t}\begin{bmatrix} v_d \\ v_q \\ v_0 \end{bmatrix} = \mathcal{W}\begin{bmatrix} v_d \\ v_q \\ v_0 \end{bmatrix} + \frac{1}{C}\begin{bmatrix} i_d \\ i_q \\ i_0 \end{bmatrix}. \tag{17}$$

Power and energy in terms of dq0 quantities

Consider a general three-phase unit as described in Fig. 3.
The instantaneous power flowing from the unit into the network at time t is

$$p_{3\phi}(t) = v_a(t)i_a(t) + v_b(t)i_b(t) + v_c(t)i_c(t). \tag{18}$$

Rewrite this equation as

$$\begin{aligned} p_{3\phi} &= \begin{bmatrix} v_a & v_b & v_c \end{bmatrix}\begin{bmatrix} i_a \\ i_b \\ i_c \end{bmatrix} = \left(T_\theta^{-1}\begin{bmatrix} v_d \\ v_q \\ v_0 \end{bmatrix}\right)^{\mathsf{T}} T_\theta^{-1}\begin{bmatrix} i_d \\ i_q \\ i_0 \end{bmatrix} \\ &= \begin{bmatrix} v_d & v_q & v_0 \end{bmatrix}\left(T_\theta^{-1}\right)^{\mathsf{T}} T_\theta^{-1}\begin{bmatrix} i_d \\ i_q \\ i_0 \end{bmatrix} \end{aligned} \tag{19}$$

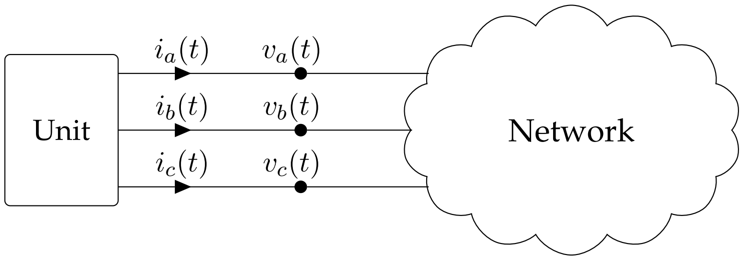

Figure 3: Three-phase unit connected to the network.

and use

$$\left(T_\theta^{-1}\right)^\mathsf{T} T_\theta^{-1} = \frac{3}{2}\begin{bmatrix}1 & 0 & 0\\ 0 & 1 & 0\\ 0 & 0 & 2\end{bmatrix} \tag{20}$$

to obtain

$$p_{3\phi} = \frac{3}{2}\begin{bmatrix}v_d & v_q & v_0\end{bmatrix}\begin{bmatrix}1 & 0 & 0\\ 0 & 1 & 0\\ 0 & 0 & 2\end{bmatrix}\begin{bmatrix}i_d\\ i_q\\ i_0\end{bmatrix} = \frac{3}{2}\left(v_d i_d + v_q i_q + 2 v_0 i_0\right). \tag{21}$$

This expression defines the three-phase instantaneous power in terms of $dq0$ quantities. Similarly, assume a symmetrically configured three-phase inductor, with currents i_a, i_b, i_c as shown in Fig. 4.

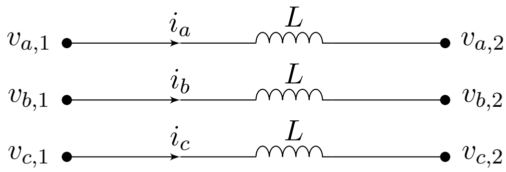

Figure 4: Symmetrically configured three-phase inductor.

The total energy stored in the inductor is

$$E = \frac{1}{2}L\left(i_a^2 + i_b^2 + i_c^2\right), \tag{22}$$

which may be written as

$$\begin{aligned} E &= \frac{1}{2}L\begin{bmatrix}i_a & i_b & i_c\end{bmatrix}\begin{bmatrix}i_a\\ i_b\\ i_c\end{bmatrix}^\mathsf{T} = \frac{1}{2}L\left(T_\theta^{-1}\begin{bmatrix}i_d\\ i_q\\ i_0\end{bmatrix}\right)^\mathsf{T} T_\theta^{-1}\begin{bmatrix}i_d\\ i_q\\ i_0\end{bmatrix}\\ &= \frac{1}{2}L\begin{bmatrix}i_d & i_q & i_0\end{bmatrix}\left(T_\theta^{-1}\right)^\mathsf{T} T_\theta^{-1}\begin{bmatrix}i_d\\ i_q\\ i_0\end{bmatrix}. \end{aligned} \tag{23}$$

Again use the identity

$$\left(T_\theta^{-1}\right)^\mathsf{T} T_\theta^{-1} = \frac{3}{2}\begin{bmatrix}1 & 0 & 0\\ 0 & 1 & 0\\ 0 & 0 & 2\end{bmatrix} \tag{24}$$

to obtain

$$E = \frac{3}{4}L\begin{bmatrix}i_d & i_q & i_0\end{bmatrix}\begin{bmatrix}1 & 0 & 0\\ 0 & 1 & 0\\ 0 & 0 & 2\end{bmatrix}\begin{bmatrix}i_d\\ i_q\\ i_0\end{bmatrix}, \tag{25}$$

which leads to

$$E = \frac{3}{4} L \left(i_d^2 + i_q^2 + 2 i_0^2 \right) . \tag{26}$$

Similarly, the energy stored in a symmetrically configured three-phase capacitor C is

$$E = \frac{3}{4} C \left(v_d^2 + v_q^2 + 2 v_0^2 \right) . \tag{27}$$

The following analysis shows that the energy derivative with respect to time is power, as expected. Consider the circuit in Fig. 4. Application of the chain rule yields

$$\frac{\mathrm{d}}{\mathrm{d}t} E = \frac{3}{2} L \left(i_d \frac{\mathrm{d} i_d}{\mathrm{d}t} + i_q \frac{\mathrm{d} i_q}{\mathrm{d}t} + 2 i_0 \frac{\mathrm{d} i_0}{\mathrm{d}t} \right) , \tag{28}$$

and based on the dynamic model of the inductor in (16) we have

$$\begin{aligned} \frac{\mathrm{d}}{\mathrm{d}t} E = \frac{3}{2} L \Bigg[& i_d \left(\frac{\mathrm{d}\theta}{\mathrm{d}t} i_q + \frac{1}{L} (v_{d,1} - v_{d,2}) \right) \\ & + i_q \left(-\frac{\mathrm{d}\theta}{\mathrm{d}t} i_d + \frac{1}{L} (v_{q,1} - v_{q,2}) \right) + 2 i_0 \left(\frac{1}{L} (v_{0,1} - v_{0,2}) \right) \Bigg] . \end{aligned} \tag{29}$$

This expression can be simplified as

$$\frac{\mathrm{d}}{\mathrm{d}t} E = \frac{3}{2} \left(v_{d,1} i_d + v_{q,1} i_q + 2 v_{0,1} i_0 \right) - \frac{3}{2} \left(v_{d,2} i_d + v_{q,2} i_q + 2 v_{0,2} i_0 \right) , \tag{30}$$

which is identical to

$$\frac{\mathrm{d}}{\mathrm{d}t} E = p_1 - p_2 . \tag{31}$$

The change in stored energy is equal to the sum of powers flowing into the inductor.

Modeling linear circuits

We will now extend the discussion in the previous section and show how to construct $dq0$ models of general three-phase circuits.

Consider a three-phase circuit composed of inductors, capacitor, resistors, voltage sources and current sources. Let x represent the state vector of this circuit in the abc reference frame, and use the compact notation $x_{abc} = [x_{a,1}, x_{b,1}, x_{c,1}, \ldots, x_{a,m}, x_{b,m}, x_{c,m}]^{\mathsf{T}}$. The circuit dynamics may be expressed as

$$\frac{\mathrm{d}}{\mathrm{d}t} x_{abc} = A x_{abc} + B u . \tag{32}$$

Define the *composite* $dq0$ transformation and its inverse as

$$\Lambda_\theta = \begin{bmatrix} T_\theta & & 0 \\ & \ddots & \\ 0 & & T_\theta \end{bmatrix} , \; \Lambda_\theta^{-1} = \begin{bmatrix} T_\theta^{-1} & & 0 \\ & \ddots & \\ 0 & & T_\theta^{-1} \end{bmatrix} , \tag{33}$$

such that $x_{dq0} = \Lambda_\theta x_{abc}$ and $x_{abc} = \Lambda_\theta^{-1} x_{dq0}$. Substitute these definitions into (32) to get

$$\frac{\mathrm{d}}{\mathrm{d}t} \left(\Lambda_\theta^{-1} x_{dq0} \right) = A \Lambda_\theta^{-1} x_{dq0} + B u , \tag{34}$$

$$\frac{\mathrm{d}}{\mathrm{d}t}\left(\Lambda_\theta^{-1}\right) x_{dq0} + \Lambda_\theta^{-1}\frac{\mathrm{d}}{\mathrm{d}t}x_{dq0} = A\Lambda_\theta^{-1}x_{dq0} + Bu. \tag{35}$$

It can be verified by direct calculations that $\frac{\mathrm{d}}{\mathrm{d}t}(\Lambda_\theta^{-1}) = -\Lambda_\theta^{-1}W_c$, where

$$W_c = \begin{bmatrix} \mathcal{W} & & 0 \\ & \ddots & \\ 0 & & \mathcal{W} \end{bmatrix}, \quad \mathcal{W} = \begin{bmatrix} 0 & \frac{\mathrm{d}}{\mathrm{d}t}\theta & 0 \\ -\frac{\mathrm{d}}{\mathrm{d}t}\theta & 0 & 0 \\ 0 & 0 & 0 \end{bmatrix}. \tag{36}$$

Substitute the expression for $\frac{\mathrm{d}}{\mathrm{d}t}(\Lambda_\theta^{-1})$ into (35) to obtain

$$-\Lambda_\theta^{-1}W_c x_{dq0} + \Lambda_\theta^{-1}\frac{\mathrm{d}}{\mathrm{d}t}x_{dq0} = A\Lambda_\theta^{-1}x_{dq0} + Bu, \tag{37}$$

and multiply from the left by Λ_θ to get

$$\frac{\mathrm{d}}{\mathrm{d}t}x_{dq0} = \left(\Lambda_\theta A \Lambda_\theta^{-1} + W_c\right) x_{dq0} + \Lambda_\theta Bu. \tag{38}$$

This equation describes the circuit dynamics based on $dq0$ quantities. In general the expression on the right depends on $\theta(t)$, and therefore this model does not have well-defined equilibrium points. However, for the special case of *symmetrically configured* networks, it is typically true that $\Lambda_\theta A = A\Lambda_\theta$, so equation (38) takes the form

$$\frac{\mathrm{d}}{\mathrm{d}t}x_{dq0} = \left(A + W_c\right) x_{dq0} + \Lambda_\theta Bu. \tag{39}$$

Under the typical assumption that the input $\Lambda_\theta Bu$ is constant, the right hand side of this equation does not include $\theta(t)$, and therefore this model has well-defined equilibrium points, and can be analyzed using standard tools.

As an example, consider the circuit in Fig. 5.

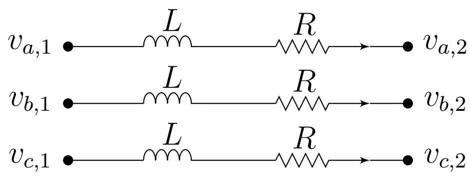

Figure 5: Example—symmetrically configured RL transmission line.

The dynamic model in the abc reference frame is

$$\frac{\mathrm{d}}{\mathrm{d}t}\begin{bmatrix} i_a \\ i_b \\ i_c \end{bmatrix} = -\frac{R}{L}\begin{bmatrix} 1 & 0 & 0 \\ 0 & 1 & 0 \\ 0 & 0 & 1 \end{bmatrix}\begin{bmatrix} i_a \\ i_b \\ i_c \end{bmatrix} + \frac{1}{L}\begin{bmatrix} v_{a,1} - v_{a,2} \\ v_{b,1} - v_{b,2} \\ v_{c,1} - v_{c,2} \end{bmatrix}. \tag{40}$$

In this example $\Lambda_\theta = T_\theta$, and therefore $W_c = \mathcal{W}$. In addition it may be verified that $T_\theta A = AT_\theta$. Based on (39) the dynamic model in the $dq0$ reference frame is

$$\frac{\mathrm{d}}{\mathrm{d}t}i_{dq0} = (A + \mathcal{W})i_{dq0} + T_\theta Bu, \tag{41}$$

which yields

$$\frac{\mathrm{d}}{\mathrm{d}t}\begin{bmatrix} i_d \\ i_q \\ i_0 \end{bmatrix} = (A + \mathcal{W})\begin{bmatrix} i_d \\ i_q \\ i_0 \end{bmatrix} + T_\theta B\begin{bmatrix} v_{a,1} - v_{a,2} \\ v_{b,1} - v_{b,2} \\ v_{c,1} - v_{c,2} \end{bmatrix}, \tag{42}$$

or equivalently

$$\frac{\mathrm{d}}{\mathrm{d}t}\begin{bmatrix} i_d \\ i_q \\ i_0 \end{bmatrix} = \left(-\frac{R}{L}\begin{bmatrix} 1 & 0 & 0 \\ 0 & 1 & 0 \\ 0 & 0 & 1 \end{bmatrix} + \begin{bmatrix} 0 & \frac{\mathrm{d}}{\mathrm{d}t}\theta & 0 \\ -\frac{\mathrm{d}}{\mathrm{d}t}\theta & 0 & 0 \\ 0 & 0 & 0 \end{bmatrix} \right) \begin{bmatrix} i_d \\ i_q \\ i_0 \end{bmatrix} + \frac{1}{L} T_\theta \begin{bmatrix} v_{a,1} - v_{a,2} \\ v_{b,1} - v_{b,2} \\ v_{c,1} - v_{c,2} \end{bmatrix}. \tag{43}$$

This last equation may be written more compactly as

$$\frac{\mathrm{d}}{\mathrm{d}t}\begin{bmatrix} i_d \\ i_q \\ i_0 \end{bmatrix} = \begin{bmatrix} -\frac{R}{L} & \frac{\mathrm{d}}{\mathrm{d}t}\theta & 0 \\ -\frac{\mathrm{d}}{\mathrm{d}t}\theta & -\frac{R}{L} & 0 \\ 0 & 0 & -\frac{R}{L} \end{bmatrix} \begin{bmatrix} i_d \\ i_q \\ i_0 \end{bmatrix} + \frac{1}{L} \begin{bmatrix} v_{d,1} - v_{d,2} \\ v_{q,1} - v_{q,2} \\ v_{0,1} - v_{0,2} \end{bmatrix}. \tag{44}$$

In addition, if the reference angle is $\theta = \omega_s t$ then

$$\frac{\mathrm{d}}{\mathrm{d}t}\begin{bmatrix} i_d \\ i_q \\ i_0 \end{bmatrix} = \begin{bmatrix} -\frac{R}{L} & \omega_s & 0 \\ -\omega_s & -\frac{R}{L} & 0 \\ 0 & 0 & -\frac{R}{L} \end{bmatrix} \begin{bmatrix} i_d \\ i_q \\ i_0 \end{bmatrix} + \frac{1}{L} \begin{bmatrix} v_{d,1} - v_{d,2} \\ v_{q,1} - v_{q,2} \\ v_{0,1} - v_{0,2} \end{bmatrix}. \tag{45}$$

The resulting model is linear and time-invariant.

How does this model change if the circuit is not symmetrically configured?

Consider a modified circuit in which the inductances are L, L, and $2L$. In this case the equality $\Lambda_\theta A = A\Lambda_\theta$ no longer holds, and therefore the dynamic model is nonlinear and time-varying, since the term $\Lambda_\theta A \Lambda_\theta^{-1}$ varies with $\theta(t)$. In this example the $dq0$ transformation does not offer any obvious advantage in comparison to direct analysis in the abc reference frame.

As another example consider the circuit in Fig. 6. The voltage sources on the left represent the secondary side of a transformer, and the voltage sources on the right represent the primary side of another transformer. The objective here is to study the effects of $R_{g,1}$ and $R_{g,2}$ on the system dynamics.

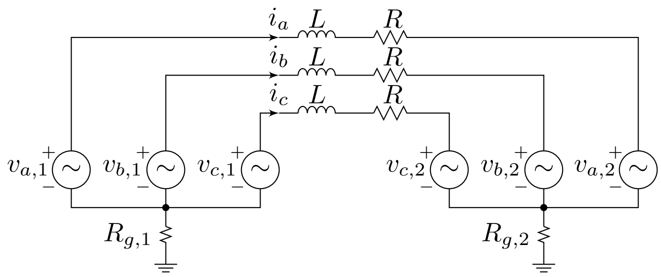

Figure 6: Example — a linear three-phase circuit.

The model in the abc reference frame is

$$\begin{aligned} L\frac{\mathrm{d}}{\mathrm{d}t}i_a &= -Ri_a - (R_{g,1} + R_{g,2})(i_a + i_b + i_c) + (v_{a,1} - v_{a,2}), \\ L\frac{\mathrm{d}}{\mathrm{d}t}i_b &= -Ri_b - (R_{g,1} + R_{g,2})(i_a + i_b + i_c) + (v_{b,1} - v_{b,2}), \\ L\frac{\mathrm{d}}{\mathrm{d}t}i_c &= -Ri_c - (R_{g,1} + R_{g,2})(i_a + i_b + i_c) + (v_{c,1} - v_{c,2}), \end{aligned} \tag{46}$$

and direct computations yield

$$\Lambda_\theta A \Lambda_\theta^{-1} = \begin{bmatrix} -\frac{R}{L} & 0 & 0 \\ 0 & -\frac{R}{L} & \\ 0 & 0 & -\frac{R+3(R_{g,1}+R_{g,2})}{L} \end{bmatrix}. \tag{47}$$

Based on (38) and assuming $\mathrm{d}\theta/\mathrm{d}t = \omega_s$ the resulting $dq0$ model is

$$\begin{aligned}
\frac{\mathrm{d}}{\mathrm{d}t} i_d &= -\frac{R}{L} i_d + \omega_s i_q + \frac{1}{L}(v_{d,1} - v_{d,2}), \\
\frac{\mathrm{d}}{\mathrm{d}t} i_q &= -\omega_s i_d - \frac{R}{L} i_q + \frac{1}{L}(v_{q,1} - v_{q,2}), \\
\frac{\mathrm{d}}{\mathrm{d}t} i_0 &= -\frac{1}{L}(R + 3(R_{g,1} + R_{g,2})) i_0 + \frac{1}{L}(v_{0,1} - v_{0,2}).
\end{aligned} \tag{48}$$

Note that in this example $\Lambda_\theta A \neq A \Lambda_\theta$, but nevertheless the $dq0$ model is linear and time-invariant.

The expressions for i_d, i_q are exactly identical to the ones in (45), and are unaffected by the resistors $R_{g,1}$ and $R_{g,2}$. These resistors affect only the zero component, which according to (1) represents the average current $i_0 = \frac{1}{3}(i_a + i_b + i_c)$. Note that if $R_{g,1} + R_{g,2} \to \infty$ then $i_0 \to 0$, but i_d, i_q are unaffected. This example may explain how transformers are used to eliminate undesired average currents in a power system.

Comparison of phasors and dq0 quantities

This section discusses the relations between $dq0$ models and time-varying phasor models. First we will define the link between phasors and $dq0$ quantities. Consider the balanced three-phase voltage signals

$$\begin{aligned}
v_a(t) &= A(t) \cos\left(\omega_s t + \psi(t)\right), \\
v_b(t) &= A(t) \cos\left(\omega_s t + \psi(t) - \frac{2\pi}{3}\right), \\
v_c(t) &= A(t) \cos\left(\omega_s t + \psi(t) + \frac{2\pi}{3}\right).
\end{aligned} \tag{49}$$

Based on the $dq0$ transformation in (2) with $\theta(t) = \omega_s t$, and using the trigonometric identity $\cos(\alpha + \beta) = \cos(\alpha)\cos(\beta) - \sin(\alpha)\sin(\beta)$ we have

$$\begin{aligned}
\begin{bmatrix} v_d \\ v_q \\ v_0 \end{bmatrix} &= T_{\omega_s t} \begin{bmatrix} v_a \\ v_b \\ v_c \end{bmatrix} = T_{\omega_s t} \begin{bmatrix} A(t)\cos\left(\omega_s t + \psi(t)\right) \\ A(t)\cos\left(\omega_s t + \psi(t) - \frac{2\pi}{3}\right) \\ A(t)\cos\left(\omega_s t + \psi(t) + \frac{2\pi}{3}\right) \end{bmatrix} \\
&= T_{\omega_s t} \begin{bmatrix} \cos\left(\omega_s t\right) & -\sin\left(\omega_s t\right) & 1 \\ \cos\left(\omega_s t - \frac{2\pi}{3}\right) & -\sin\left(\omega_s t - \frac{2\pi}{3}\right) & 1 \\ \cos\left(\omega_s t + \frac{2\pi}{3}\right) & -\sin\left(\omega_s t + \frac{2\pi}{3}\right) & 1 \end{bmatrix} \begin{bmatrix} A(t)\cos\left(\psi(t)\right) \\ A(t)\sin\left(\psi(t)\right) \\ 0 \end{bmatrix} \\
&= T_{\omega_s t} T_{\omega_s t}^{-1} \begin{bmatrix} A(t)\cos\left(\psi(t)\right) \\ A(t)\sin\left(\psi(t)\right) \\ 0 \end{bmatrix} = \begin{bmatrix} A(t)\cos\left(\psi(t)\right) \\ A(t)\sin\left(\psi(t)\right) \\ 0 \end{bmatrix},
\end{aligned} \tag{50}$$

and therefore

$$\begin{aligned}
v_d(t) &= A(t)\cos(\psi(t)), \\
v_q(t) &= A(t)\sin(\psi(t)) \\
v_0(t) &= 0.
\end{aligned} \tag{51}$$

In addition, assuming that variations in the magnitude $A(t)$ and phase $\psi(t)$ are "slow" (see definition below) in comparison to the nominal system frequency ω_s, the voltages above may be represented by the time-varying phasor

$$V(t) = \frac{A(t)}{\sqrt{2}} e^{j\psi(t)}. \tag{52}$$

Following (51) and (52) the phasor $V(t)$ may be expressed in terms of $dq0$ quantities as

$$\begin{aligned} V(t) &= \frac{A(t)}{\sqrt{2}} e^{j\psi(t)} = \frac{A(t)}{\sqrt{2}} \left(\cos(\psi(t)) + j\sin(\psi(t))\right) \\ &= \frac{1}{\sqrt{2}} \left(v_d(t) + jv_q(t)\right), \end{aligned} \tag{53}$$

or alternatively,

$$v_d(t) = \sqrt{2}\,\mathrm{Re}\{V(t)\}, \quad v_q(t) = \sqrt{2}\,\mathrm{Im}\{V(t)\} \quad v_0(t) = 0. \tag{54}$$

Note that since $v_0(t) = 0$ this definition holds only for balanced three-phase signals. Similarly the active power, reactive power, amplitude and phase may be defined with respect to the dq components as follows:

$$\begin{aligned} P(t) &= \mathrm{Re}\left\{V(t)I^*(t)\right\} = \frac{1}{2}\left(v_d(t)i_d(t) + v_q(t)i_q(t)\right), \\ Q(t) &= \mathrm{Im}\left\{V(t)I^*(t)\right\} = \frac{1}{2}\left(v_q(t)i_d(t) - v_d(t)i_q(t)\right), \\ |V(t)|^2 &= \mathrm{Re}\left\{V(t)\right\}^2 + \mathrm{Im}\left\{V(t)\right\}^2 = \frac{1}{2}\left(v_d^2(t) + v_q^2(t)\right), \\ \angle V(t) &= \mathrm{atan2}(v_q, v_d). \end{aligned} \tag{55}$$

We will now examine the similarities and differences between $dq0$ models and time-varying phasor models. Consider the symmetrically configured inductor, which dynamic model is given in (16). Assuming $\theta = \omega_s t$ and $v_0 = 0$ this model may be written as

$$\begin{aligned} v_d(t) &= -\omega_s L i_q(t) + L\frac{\mathrm{d}}{\mathrm{d}t} i_d, \\ v_q(t) &= \omega_s L i_d(t) + L\frac{\mathrm{d}}{\mathrm{d}t} i_q. \end{aligned} \tag{56}$$

Using time-varying phasors the inductor impedance is $j\omega_s L$, and therefore

$$I(t) = \frac{1}{j\omega_s L} V(t), \tag{57}$$

where $V(t)$ and $I(t)$ are the phasors representing the inductor voltage and current. The real and imaginary parts of this last equation are

$$\begin{aligned} \mathrm{Re}\{I(t)\} &= \frac{1}{\omega_s L}\,\mathrm{Im}\{V(t)\}, \\ \mathrm{Im}\{I(t)\} &= -\frac{1}{\omega_s L}\,\mathrm{Re}\{V(t)\}, \end{aligned} \tag{58}$$

and based on the relations between dq signals and phasors in (54) an equivalent model is

$$\begin{aligned} i_d(t) &= \frac{1}{\omega_s L} v_q(t), \\ i_q(t) &= -\frac{1}{\omega_s L} v_d(t), \end{aligned} \tag{59}$$

or

$$\begin{aligned} v_d(t) &= -\omega_s L i_q(t), \\ v_q(t) &= \omega_s L i_d(t). \end{aligned} \tag{60}$$

Direct comparison of (56) and (60) reveals that both models are similar, except for the time derivatives in the $dq0$ model. These derivatives describe the main difference between the two models. While the $dq0$ model is general and accurate, the time-varying phasor model is an approximation, which only holds for slow variations. If variations in the dq components are indeed slow such that

$$\begin{aligned} \left|\frac{\mathrm{d}}{\mathrm{d}t} i_d\right| &<< \omega_s \left|i_q(t)\right|, \\ \left|\frac{\mathrm{d}}{\mathrm{d}t} i_q\right| &<< \omega_s \left|i_d(t)\right|, \end{aligned} \tag{61}$$

then (56) and (60) are almost identical, and therefore time-varying phasors may be used instead of $dq0$ quantities. This result is extended in [1] and [2], which formulate the relations between $dq0$ models and time varying phasor models for general three-phase networks.

Remark (Equilibrium points): for balanced systems, since at equilibrium the time derivatives are equal to zero, the $dq0$ model is identical to the time-varying phasor model. For this reason equilibrium points may be calculated based on phasors. This is typically done by solving the system's power flow equations, as described in Lecture 1.

Power expressions for phasors and for dq0 quantities

In this section we will briefly recall the power definitions we developed so far, and examine how they relate to each other.

Equation (21) defines the *instantaneous three-phase* power:

$$p_{3\phi}(t) = v_a(t)i_a(t) + v_b(t)i_b(t) + v_c(t)i_c(t) = \frac{3}{2}\left(v_d(t)i_d(t) + v_q(t)i_q(t) + 2v_0(t)i_0(t)\right). \tag{62}$$

In addition, in the context of time-varying phasor models we discussed the *active* power:

$$P(t) = \frac{1}{T}\int_{t-T/2}^{t+T/2} v_a(\tau)i_a(\tau)\mathrm{d}\tau = \frac{1}{T}\int_{t-T/2}^{t+T/2} v_b(\tau)i_b(\tau)\mathrm{d}\tau = \frac{1}{T}\int_{t-T/2}^{t+T/2} v_c(\tau)i_c(\tau)\mathrm{d}\tau. \tag{63}$$

Here $v_a i_a$, $v_b i_b$, $v_c i_c$ are the instantaneous single-phase powers, and T is the period of the AC signals. The active power is the *average* power over a cycle, for a single phase. We have also seen in (55) that under the approximation of time varying phasors

$$\begin{aligned} P(t) &= \mathrm{Re}\left\{V(t)I^*(t)\right\} = \frac{1}{2}\left(v_d(t)i_d(t) + v_q(t)i_q(t)\right), \\ Q(t) &= \mathrm{Im}\left\{V(t)I^*(t)\right\} = \frac{1}{2}\left(v_q(t)i_d(t) - v_d(t)i_q(t)\right). \end{aligned} \tag{64}$$

Based on (62) and (64) and assuming that in a balanced power system $v_0 = 0$ we have

$$p_{3\phi}(t) = 3P(t), \tag{65}$$

which means that the *total instantaneous* power is equal to three times the *active* power.

Moreover, the approximation of time-varying phasors dictates that variations in $P(t)$ during a single cycle are small. Therefore, based on (65), the total instantaneous power $p_{3\phi}(t)$ must be almost constant during a cycle. This fact is one of the greatest advantages of balanced three-phase systems. While a single-phase system provides alternating power, a balanced three-phase system provides almost constant power. As a result, three-phase devices do not need to store significant energy, and can be made small and efficient. This idea is illustrated in Fig. 7.

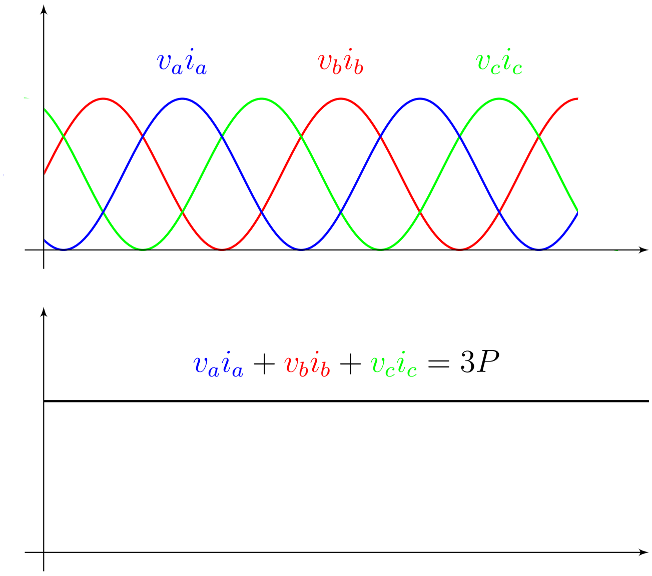

Figure 7: While a single-phase system provides alternating power, a balanced three-phase system provides nearly constant power.

Example — modeling a network based on dq0 quantities

Consider the linear three-phase network described in Fig. 8. The network includes an ideal power source which is connected to an infinite bus (a voltage source with constant amplitude and frequency).

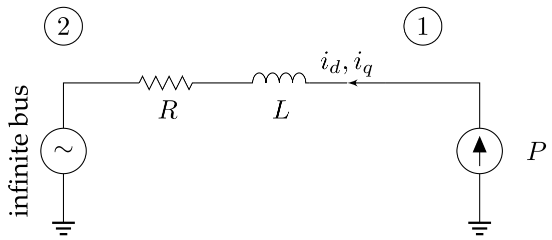

Figure 8: Ideal power source connected to an infinite bus (single-phase diagram).

It is assumed that

- ✓ The network and the sources within it are symmetrically configured;
- ✓ the reference angle for the $dq0$ transformation is $\theta = \omega_s t$, where ω_s is the frequency of the infinite bus.
- ✓ The power source is modeled as

$$\begin{aligned} &\frac{1}{2}(v_{d,1} i_d + v_{q,1} i_q) = P, \\ &\frac{1}{2}(v_{q,1} i_d - v_{d,1} i_q) = 0, \\ &v_{0,1} = 0. \end{aligned} \tag{66}$$

- ✓ The infinite bus is modeled as

$$\begin{aligned} v_{d,2} &= \sqrt{2} V_g, \\ v_{q,2} &= 0, \\ v_{0,2} &= 0. \end{aligned} \tag{67}$$

Time-varying phasor model

Here it is assumed that the network may be described based on time-varying phasors. The voltage of the infinite bus is

$$V_2 = V_g, \tag{68}$$

and the power source is characterized by

$$\begin{aligned} P_1 &= P, \\ Q_1 &= 0, \end{aligned} \tag{69}$$

where V_g and P are given constants.

We define the inductor current as I, and the voltage on the power source as V_1 (these are phasors). The system equations are

$$\begin{aligned} P &= V_1 I^*, \\ V_1 - V_g &= (j\omega_s L + R)I, \end{aligned} \tag{70}$$

which lead to

$$\begin{aligned} P &= (V_g + (j\omega_s L + R)I)\, I^* \\ &= V_g I^* + (j\omega_s L + R)|I|^2. \end{aligned} \tag{71}$$

This last equation may be solved to find the current I.

It can be seen that the time-varying phasor model has no dynamic states, and is characterized by a set of algebraic equations. The solution, if it exists, is constant in time.

DQ0 model

We will now develop the $dq0$ model of the network above assuming that $R = 0$.

According to (16) with $\theta = \omega_s t$ the inductor model is

$$\begin{aligned} \frac{\mathrm{d}}{\mathrm{d}t} i_d &= \omega_s i_q + \frac{1}{L}(v_{d,1} - v_{d,2}), \\ \frac{\mathrm{d}}{\mathrm{d}t} i_q &= -\omega_s i_d + \frac{1}{L}(v_{q,1} - v_{q,2}). \end{aligned} \tag{72}$$

The power source is modeled as in (66), which may be written as

$$\begin{bmatrix} v_{d,1} \\ v_{q,1} \end{bmatrix} = \frac{2P}{i_d^2 + i_q^2} \begin{bmatrix} i_d \\ i_q \end{bmatrix}. \tag{73}$$

Combination of (67), (72) and (73) yields the (nonlinear) state-space model

$$\begin{aligned} \frac{\mathrm{d}}{\mathrm{d}t} i_d &= \omega_s i_q + \frac{2P}{L}\frac{i_d}{i_d^2 + i_q^2} - \frac{\sqrt{2}V_g}{L}, \\ \frac{\mathrm{d}}{\mathrm{d}t} i_q &= -\omega_s i_d + \frac{2P}{L}\frac{i_q}{i_d^2 + i_q^2}, \end{aligned} \tag{74}$$

which Jacobian at an equilibrium point $(\bar{i}_d, \bar{i}_q)$ is

$$A = \begin{bmatrix} -\frac{2P}{L}\frac{\bar{i}_d^2 - \bar{i}_q^2}{\left(\bar{i}_d^2 + \bar{i}_q^2\right)^2} & \omega_s - \frac{4P}{L}\frac{\bar{i}_d \bar{i}_q}{\left(\bar{i}_d^2 + \bar{i}_q^2\right)^2} \\ -\omega_s - \frac{4P}{L}\frac{\bar{i}_d \bar{i}_q}{\left(\bar{i}_d^2 + \bar{i}_q^2\right)^2} & \frac{2P}{L}\frac{\bar{i}_d^2 - \bar{i}_q^2}{\left(\bar{i}_d^2 + \bar{i}_q^2\right)^2} \end{bmatrix}. \tag{75}$$

The poles are found by computing the roots of the characteristic polynomial, which is given for a second-order system by

$$s^2 - \mathrm{Tr}(A)s + \det(A) = 0, \tag{76}$$

where $\mathrm{Tr}(A)$ is the trace of A, and $\det(A)$ is the determinant of A. It is easy to verify that in our example $\mathrm{Tr}(A) = 0$, and therefore the poles are $s_{1,2} = \pm\sqrt{\det(A)}$. Consider the following two cases:

- ✓ If $\det(A) > 0$ there is a pole in the right half of the complex plane, and the system is unstable.
- ✓ If $\det(A) \leq 0$ there is a complex conjugate pair of poles on the imaginary axis, and additional analysis in simulation reveals that the system is unstable.

Based on these results we can conclude that the $dq0$ model is unstable.

Can we use the approximation of time-varying phasors in this example? We have seen that

- ✓ The time-varying phasor model has no dynamic states, and therefore provides no information regarding the system stability.
- ✓ With $R = 0$ the $dq0$ model is unstable.

The time-varying phasor model may be used to find the equilibrium point(s). However, in case $R = 0$, the $dq0$ model reveals that these equilibrium points are unstable, and do not represent physical solutions.

Work [3] considers the same example with an additional capacitor which is connected in parallel to the power source. This additional capacitor acts as an energy storage device, and may help to stabilize the system.

Appendix: useful dq0 identities

Here are several useful identities related to the $dq0$ transformation.

$$T_\theta = \frac{2}{3}\begin{bmatrix} \cos(\theta) & \cos\left(\theta - \frac{2\pi}{3}\right) & \cos\left(\theta + \frac{2\pi}{3}\right) \\ -\sin(\theta) & -\sin\left(\theta - \frac{2\pi}{3}\right) & -\sin\left(\theta + \frac{2\pi}{3}\right) \\ \frac{1}{2} & \frac{1}{2} & \frac{1}{2} \end{bmatrix}, \tag{77}$$

$$T_\theta^{-1} = \begin{bmatrix} \cos(\theta) & -\sin(\theta) & 1 \\ \cos\left(\theta - \frac{2\pi}{3}\right) & -\sin\left(\theta - \frac{2\pi}{3}\right) & 1 \\ \cos\left(\theta + \frac{2\pi}{3}\right) & -\sin\left(\theta + \frac{2\pi}{3}\right) & 1 \end{bmatrix}, \tag{78}$$

$$T_\theta T_\theta^{-1} = T_\theta^{-1} T_\theta = I_{3\times 3}, \tag{79}$$

$$\left(T_\theta^{-1}\right)^{\mathsf{T}} T_\theta^{-1} = \frac{3}{2}\begin{bmatrix} 1 & 0 & 0 \\ 0 & 1 & 0 \\ 0 & 0 & 2 \end{bmatrix}, \tag{80}$$

$$T_\theta \left(T_\theta\right)^{\mathsf{T}} = \frac{2}{3}\begin{bmatrix} 1 & 0 & 0 \\ 0 & 1 & 0 \\ 0 & 0 & \frac{1}{2} \end{bmatrix}, \tag{81}$$

$$T_{\theta_a} T_{\theta_b}^{-1} = \begin{bmatrix} \cos(\theta_a - \theta_b) & \sin(\theta_a - \theta_b) & 0 \\ -\sin(\theta_a - \theta_b) & \cos(\theta_a - \theta_b) & 0 \\ 0 & 0 & 1 \end{bmatrix}, \tag{82}$$

$$\begin{aligned} \frac{\mathrm{d}}{\mathrm{d}t} T_\theta^{-1} &= -T_\theta^{-1} \mathcal{W}, \\ \frac{\mathrm{d}}{\mathrm{d}t} T_\theta &= \mathcal{W} T_\theta, \end{aligned} \tag{83}$$

with

$$\mathcal{W} = \begin{bmatrix} 0 & \frac{\mathrm{d}}{\mathrm{d}t}\theta & 0 \\ -\frac{\mathrm{d}}{\mathrm{d}t}\theta & 0 & 0 \\ 0 & 0 & 0 \end{bmatrix}. \tag{84}$$

All these identities can be proved by straight-forward algebraic calculations.

References

[1] Y. Levron and J. Belikov, "Modeling power networks using dynamic phasors in the dq0 reference frame," *Electric Power Systems Research*, vol. 144, pp. 233–242, Mar. 2017.

[2] J. Belikov and Y. Levron, "Comparison of time-varying phasor and dq0 dynamic models for large transmission networks," *International Journal of Electrical Power & Energy Systems*, vol. 93, pp. 65–74, 2017.

[3] A. Fahima, R. Ofir, J. Belikov, and Y. Levron, "Minimal energy storage required for stability of low inertia distributed sources," in *International Energy Conference*, Limassol, Cyprus, 2018, pp. 1–5.

[4] D. Baimel, J. Belikov, J. M. Guerrero, and Y. Levron, "Dynamic modeling of networks, microgrids, and renewable sources in the dq0 reference frame: A survey," *IEEE Access*, vol. 5, pp. 21 323–21 335, 2017.

[5] P. M. Anderson and A. A. Fouad, *Power System Control and Stability*. John Wiley & Sons, 2008.

[6] J. H. Chow, *Power System Coherency and Model Reduction*. Springer, 2013.

[7] J. J. Grainger and W. D. Stevenson, *Power System Analysis*. New York: McGraw-Hill, 1994.

[8] M. Ilić and J. Zaborszky, *Dynamics and Control of Large Electric Power Systems*. New York: Wiley, 2000.

[9] J. Machowski, J. Bialek, and J. Bumby, *Power Dystem Dynamics: Stability and Control*. John Wiley & Sons, 2011.

[10] W. D. Stevenson, *Elements of Power System Analysis*, 4th ed., ser. Electrical and Electronic Engineering Series, F. E. Terman, Ed. New York: McGraw-Hill, 1982.

[11] R. Teodorescu, M. Liserre, and P. Rodriguez, *Grid Converters for Photovoltaic and Wind Power Systems*. John Wiley & Sons, 2011.

[12] Q. C. Zhong and T. Hornik, *Control of Power Inverters in Renewable Energy and Smart Grid Integration*. New York, USA: John Wiley & Sons, 2013.

[13] P. Kundur, *Power system stability and control*. McGraw-Hill, 1994.

[14] P. W. Sauer and M. A. Pai, *Power system dynamics and stability*. Upper Saddle River, New Jersey: Prentice Hall, 1998.

[15] J. Belikov and Y. Levron, "Uses and misuses of quasi-static models in modern power systems," *IEEE Transactions on Power Delivery*, 2018.

[16] Y. Levron and D. Shmilovitz, "Optimal power management in fueled systems with finite storage capacity," *IEEE Transactions on Circuits and Systems I: Regular Papers*, vol. 57, no. 8, pp. 2221–2231, 2010.

[17] Y. Levron and J. Belikov, "Observable canonical forms of multi-machine power systems using dq0 signals," in *IEEE International Conference on the Science of Electrical Engineering*, 2016, pp. 1–6.

[18] Y. Levron and J. Belikov, "Open-source software for modeling and analysis of power networks in the dq0 reference frame," in *IEEE PES PowerTech Conference*, 2017, pp. 1–6.

[19] Y. Levron and J. Belikov, "DQ0 dynamics," 2017. [Online]. Available: https://a-lab.ee/projects/dq0-dynamics

[20] J. Belikov and Y. Levron, "A sparse minimal-order dynamic model of power networks based on dq0 signals," *IEEE Transactions on Power Systems*, vol. 33, no. 1, pp. 1059–1067, 2018.

[21] J. Belikov and Y. Levron, "Dynamic modeling and stability analysis of power networks using dq0 transformations with a unified reference frame," *Proceedings of the Estonian Academy of Sciences*, vol. 67, no. 4, pp. 368–377, 2018.

[22] J. Belikov and Y. Levron, "Integration of long transmission lines in large-scale dq0 dynamic models," *Electrical Engineering*, vol. 100, no. 2, pp. 1219–1228, 2018.

[23] J. Belikov and Y. Levron, "Uses and misuses of quasi-static models in modern power systems," *IEEE Transactions on Power Delivery*, vol. 33, no. 6, pp. 3263–3266, 2018.

[24] Y. Levron, J. Belikov, and D. Baimel, "A tutorial on dynamics and control of power systems with distributed and renewable energy sources based on the DQ0 transformation," *Applied Sciences*, vol. 8, no. 9, pp. 1–48, 2018.

[25] T. Demiray and G. Andersson, "Comparison of the efficiency of dynamic phasor models derived from ABC and DQ0 reference frame in power system dynamic simulations," in *The 7th IET International Conference on Advances in Power System Control, Operation and Management*, 2006, pp. 1–8.

[26] Y. Du, J. Su, M. Mao, and X. Yang, "Autonomous controller based on synchronous generator dq0 model for micro grid inverters," in *The 8th International Conference on Power Electronics*, 2011, pp. 2645–2649.

[27] W. Liu and Z. Cai, "Model analysis and robust control design of VSC-HVDC converter with dq0 axis," in *Third International Conference on Electric Utility Deregulation and Restructuring and Power Technologies*, 2008, pp. 1792–1796.

[28] A. Medina and R. Cisneros, "Power quality assessment with a state space model of a wind park in dq0 coordinates," in *Electrical Power & Energy Conference*, 2009, pp. 1–6.

[29] J. Moia, A. J. Perin, and M. L. Heldwein, "Neutral point clamped converter DC-link center point current analysis in the dq0 reference frame," in *Brazilian Power Electronics Conference*, 2011, pp. 121–128.

[30] E. R. Sanagiotti, A. A. Oliveira, J. R. B. A. Monteiro, and M. L. De Aguiar, "A comparative study between symmetrical two-phase induction motor model using dq0 transformation and model using spiral vector theory operating under unbalanced voltage," in *Conference on Industrial Electronics and Applications*, 2007, pp. 1504–1508.

[31] M. F. Schonardie, R. F. Coelho, R. Schweitzer, and D. C. Martins, "Control of the active and reactive power using dq0 transformation in a three-phase grid-connected PV system," in *IEEE International Symposium on Industrial Electronics*, 2012, pp. 264–269.

[32] M. F. Schonardie and D. C. Martins, "Application of the dq0 transformation in the three-phase grid-connected PV systems with active and reactive power control," in *IEEE International Conference on Sustainable Energy Technologies*, 2008, pp. 18–23.

[33] M. F. Schonardie and D. C. Martins, "Three-phase grid-connected photovoltaic system with active and reactive power control using dq0 transformation," in *IEEE Power Electronics Specialists Conference*, 2008, pp. 1202–1207.

[34] M. F. Schonardie, A. Ruseler, R. F. Coelho, and D. C. Martins, "Three-phase grid-connected PV system with active and reactive power control using dq0 transformation," in *The 9th IEEE/IAS International Conference on Industry Applications*, 2010, pp. 1–6.

[35] P. Szcześniak, Z. Fedyczak, and M. Klytta, "Modelling and analysis of a matrix-reactance frequency converter based on buck-boost topology by DQ0 transformation," in *The 13th International Power Electronics and Motion Control Conference*, 2008, pp. 165–172.

[36] R. Crosier and S. Wang, "DQ-frame modeling of an active power filter integrated with a grid-connected, multifunctional electric vehicle charging station," *IEEE Transactions on Power Electronics*, vol. 28, no. 12, pp. 5702–5716, 2013.

[37] M. Fasil, C. Antaloae, N. Mijatovic, B. B. Jensen, and J. Holboll, "Improved dq-axes model of PMSM considering airgap flux harmonics and saturation," *IEEE Transactions on Applied Superconductivity*, vol. 26, no. 4, pp. 1–5, 2016.

[38] C. Finotti and E. Gaio, "Continuous model in dq frame of thyristor controlled reactors for stability analysis of high power electrical systems," *International Journal of Electrical Power & Energy Systems*, vol. 63, pp. 836–845, 2014.

[39] C. Finotti, E. Gaio, I. Benfatto, I. Song, and J. Tao, "Continuous state-space model in dq frame of the thyristor AC/DC converters for stability analysis of ITER pulsed power electrical system," *IEEE Transactions on Plasma Science*, vol. 44, no. 11, pp. 2923–2931, 2016.

[40] A. Jamshidifar and D. Jovcic, "Small-signal dynamic DQ model of modular multilevel converter for system studies," *IEEE Transactions on Power Delivery*, vol. 31, no. 1, pp. 191–199, 2016.

[41] B. K. Perkins and M. R. Iravani, "Dynamic modeling of high power static switching circuits in the dq-frame," *IEEE Transactions on Power Systems*, vol. 14, no. 2, pp. 678–684, 1999.

[42] J. Poza, E. Oyarbide, D. Roye, and M. Rodriguez, "Unified reference frame dq model of the brushless doubly fed machine," *IEE Proceedings-Electric Power Applications*, vol. 153, no. 5, pp. 726–734, 2006.

[43] M. Rasheduzzaman, J. A. Mueller, and J. W. Kimball, "An accurate small-signal model of inverter-dominated islanded microgrids using dq reference frame," *IEEE Journal of Emerging and Selected Topics in Power Electronics*, vol. 2, no. 4, pp. 1070–1080, 2014.

[44] R. Reginatto and R. A. Ramos, "On electrical power evaluation in dq coordinates under sinusoidal unbalanced conditions," *IET Generation, Transmission & Distribution*, vol. 8, no. 5, pp. 976–982, 2014.

[45] S. Golestan, M. Ramezani, J. M. Guerrero, and M. Monfared, "dq-frame cascaded delayed signal cancellation-based PLL: analysis, design, and comparison with moving average filter-based PLL," *IEEE Transactions on Power Electronics*, vol. 30, no. 3, pp. 1618–1632, 2015.

[46] A. Zulu, B. C. Mecrow, and M. Armstrong, "Investigation of the dq-equivalent model for performance prediction of flux-switching synchronous motors with segmented rotors," *IEEE Transactions on Industrial Electronics*, vol. 59, no. 6, pp. 2393–2402, 2012.

[47] S.-B. Han, N.-S. Choi, C.-T. Rim, and G.-H. Cho, "Modeling and analysis of static and dynamic characteristics for buck-type three-phase PWM rectifier by circuit DQ transformation," *IEEE Transactions on Power Electronics*, vol. 13, no. 2, pp. 323–336, 1998.

[48] B. Bahrani, A. Karimi, B. Rey, and A. Rufer, "Decoupled dq-current control of grid-tied voltage source converters using nonparametric models," *IEEE Transactions on Industrial Electronics*, vol. 60, no. 4, pp. 1356–1366, 2013.

[49] B. Bahrani, S. Kenzelmann, and A. Rufer, "Multivariable-PI-based dq current control of voltage source converters with superior axis decoupling capability," *IEEE Transactions on Industrial Electronics*, vol. 58, no. 7, pp. 3016–3026, 2011.

[50] S. T. Kalyani and G. T. Das, "Simulation of DQ control system for a unified power flow controller," *ARPN Journal of Engineering and Applied Sciences*, vol. 2, no. 6, pp. 10–19, 2007.

[51] A. S. Abdel-khalik, S. Ahmed, and A. Massoud, "A five-phase induction machine model using multiple dq planes considering the effect of magnetic saturation," in *Energy Conversion Congress and Exposition*, 2014, pp. 287–293.

[52] K.-N. Areerak, S. V. Bozhko, G. M. Asher, and D. W. P. Thomas, "Stability analysis and modelling of AC-DC system with mixed load using DQ-transformation method," in *International Symposium on Industrial Electronics*, 2008, pp. 19–24.

[53] A. Bodrov, Y. Nauel, R. Todd, and J. Apsley, "Equivalence of generalized state-space averaging with DQ modelling methods in a balanced three-phase system," in *Energy Conversion Congress and Exposition*, 2015, pp. 5519–5524.

[54] K. Chaijarurnudomrung, K. N. Areerak, and K. L. Areerak, "Modeling of three-phase controlled rectifier using a DQ method," in *International Conference on Advances in Energy Engineering*, 2010, pp. 56–59.

[55] R. Crosier, S. Wang, and Y. Chu, "Modeling of a grid-connected, multifunctional electric vehicle charging station in active filter mode with DQ theory," in *Energy Conversion Congress and Exposition*, 2012, pp. 3395–3402.

[56] M. Farshadnia, M. A. M. Cheema, R. Dutta, J. E. Fletcher, H. C. Lovatt, and M. F. Rahman, "An extended dq model for concentrated-wound interior permanent magnet machines considering non-ideal machine parameters," in *International Conference on Power Electronics, Machines and Drives*, 2016, pp. 1–6.

[57] S.-B. Han, N.-S. Choi, C. t. Rim, and G.-H. Cho, "Modeling and analysis of buck type three phase PWM rectifier by circuit DQ transformation," in *The 26th Annual IEEE Power Electronics Specialists Conference*, 1995, pp. 431–436.

[58] Q. Lei, S. Liang, F. Z. Peng, M. Shen, and V. Blasko, "A generalized DQ impedance model of three phase diode rectifier," in *Energy Conversion Congress and Exposition*, 2013, pp. 3340–3347.

[59] Q. Lei, M. Shen, V. Blasko, S. Liang, and F. Z. Peng, "A generalized DQ impedance model of ATRU system," in *Twenty-Ninth Annual IEEE Applied Power Electronics Conference and Exposition*, 2014, pp. 1874–1881.

[60] W.-X. Lin and D. Jovcic, "High-power high-frequency converter modelling using Dommel's and Runge-Kutta methods in ABC and DQ frame," in *PES General Meeting | Conference & Exposition*, 2014, pp. 1–5.

[61] W. Lin and D. Jovcic, "Modelling of VSC converters in the rotating dq frame for DC fault," in *International Conference on AC and DC Power Transmission*, 2015, pp. 1–6.

[62] J. Liu and W. Chen, "Generalized DQ model of the permanent magnet synchronous motor based on extended Park transformation," in *International Future Energy Electronics Conference*, 2013, pp. 885–890.

[63] T. Messo, A. Aapro, and T. Suntio, "Generalized multivariable small-signal model of three-phase grid-connected inverter in DQ-domain," in *IEEE 16th Workshop on Control and Modeling for Power Electronics*, 2015, pp. 1–8.

[64] M. Nemec, K. Drobnič, H. Lavrič, and V. Ambrožič, "Evaluation of simplified dq model of induction machine for development of diagnostic procedures," in *The 8th International Conference on Compatibility and Power Electronics*, 2013, pp. 250–254.

[65] S. C. S. Rao and R. M. Cuzner, "Capacitor excited single phase brushless generator design and modelling using dq variables," in *International Conference on Power Electronics, Drives and Energy Systems for Industrial Growth*, 1996, pp. 523–529.

[66] J. Rao, R. Qu, D. Li, and Y. Gao, "An improved dq-axis coordinate system model for interior permanent magnet machines," in *Conference on Electromagnetic Field Computation*, 2016, pp. 1–1.

[67] P. Sushma, B. L. R. R. Samaga, and K. P. Vittal, "DQ modeling of induction motor for virtual flux measurement," in *IPEC, 2010 Conference Proceedings*, 2010, pp. 903–908.

[68] Y. Tang, Z. Qin, F. Blaabjerg, and P. C. Loh, "DQ reference frame modeling and control of single-phase active power decoupling circuits," in *Applied Power Electronics Conference and Exposition*, 2015, pp. 2725–2732.

[69] T. Yali, S. Ke, and S. Miao, "AC permanent magnet electric driving system with limited power supply modeling in dq coordinate and simulation," in *International Conference on Computer Application and System Modeling*, 2010, pp. V10–600–V10–604.

[70] H. Ye, Y. Tang, and Y. Xia, "DQ-domain modeling for multi-scale transients in a synchronous machine," in *The 5th International Conference on Electric Utility Deregulation and Restructuring and Power Technologies*, 2015, pp. 285–289.

[71] A. Zulu, B. C. Mecrow, and M. Armstrong, "Prediction of performance of a wound-field segmented-rotor flux-switching synchronous motor using a dq-equivalent model," in *The XIX International Conference on Electrical Machines*, 2010, pp. 1–6.

[72] S. Golestan, M. Monfared, J. M. Guerrero, and M. Joorabian, "A DQ synchronous frame controller for single-phase inverters," in *Power Electronics, Drive Systems and Technologies Conference*, 2011, pp. 317–323.

[73] Z. Shen, M. Jaksic, B. Zhou, P. Mattavelli, D. Boroyevich, J. Verhulst, and M. Belkhayat, "Analysis of phase locked loop (PLL) influence on DQ impedance measurement in three-phase AC systems," in *Applied Power Electronics Conference and Exposition (APEC), 2013 Twenty-Eighth Annual IEEE*, 2013, pp. 939–945.

[74] N. A. Ninad and L. A. C. Lopes, "Per-phase DQ control of a three-phase battery inverter in a diesel hybrid mini-grid supplying single-phase loads," in *The International Conference on Industrial Technology*, 2011, pp. 204–209.

[75] S. D. Round, Q. Yu, L. E. Norum, and T. M. Undeland, "Performance of a unified power flow controller using a dq control system," in *Sixth International Conference on AC and DC Power Transmission*, 1996, pp. 357–362.

[76] S. Li and T. A. Haskew, "Analysis of decoupled dq vector control in DFIG back-to-back PWM converter," in *Power Engineering Society General Meeting*, 2007, pp. 1–7.

[77] S. Li and T. A. Haskew, "Transient and steady-state simulation study of decoupled dq vector control in PWM converter of variable speed wind turbines," in *The 33rd Annual Conference of the IEEE Industrial Electronics Society*, 2007, pp. 2079–2086.

[78] N. Mendalek, K. Al-Haddad, F. Fnaiech, and L. A. Dessaint, "Sliding mode control of 3-phase 3-wire shunt active filter in the dq frame," in *Canadian Conference on Electrical and Computer Engineering*, vol. 2, 2001, pp. 765–769.

[79] N. Kroutikova, C. A. Hernandez-Aramburo, and T. C. Green, "State-space model of grid-connected inverters under current control mode," *IET Electric Power Applications*, vol. 1, no. 3, pp. 329–338, 2007.

[80] P. C. Loh and D. G. Holmes, "Analysis of multiloop control strategies for LC/CL/LCL-filtered voltage-source and current-source inverters," *IEEE Transactions on Industry Applications*, vol. 41, no. 2, pp. 644–654, 2005.

[81] F. Katiraei, M. R. Iravani, and P. W. Lehn, "Small-signal dynamic model of a micro-grid including conventional and electronically interfaced distributed resources," *IET Generation, Transmission & Distribution*, vol. 1, no. 3, pp. 369–378, 2007.

[82] F. Katiraei, R. Iravani, N. Hatziargyriou, and A. Dimeas, "Microgrids management," *IEEE Power and Energy Magazine*, vol. 6, no. 3, pp. 54–65, 2008.

[83] P. C. Krause and C. H. Thomas, "Simulation of symmetrical induction machinery," *IEEE Transactions on Power Apparatus and Systems*, vol. 84, no. 11, pp. 1038–1053, 1965.

[84] P. C. Krause, O. Wasynczuk, S. D. Sudhoff, and S. Pekarek, *Analysis of Electric Machinery and Drive Systems*, 3rd ed. Wiley-IEEE Press, 2013.

[85] M. Babazadeh and H. Karimi, "Robust decentralized control for islanded operation of a microgrid," in *Power and Energy Society General Meeting*, 2011, pp. 1–8.

[86] M. S. Mahmoud, S. A. Hussainr, and M. A. Abido, "Modeling and control of microgrid: An overview," *Journal of the Franklin Institute*, vol. 351, no. 5, pp. 2822–2859, 2014.

[87] J. Schiffer, D. Zonetti, R. Ortega, A. M. Stanković, T. Sezi, and J. Raisch, "A survey on modeling of microgrids—From fundamental physics to phasors and voltage sources," *Automatica*, vol. 74, pp. 135–150, 2016.

[88] Y. Ojo and J. Schiffer, "Towards a time-domain modeling framework for small-signal analysis of unbalanced microgrids," in *The 12th IEEE PES PowerTech Conference*, 2017, pp. 1–6.

[89] P. W. Sauer, B. C. Lesieutre, and M. A. Pai, "Transient algebraic circuits for power system dynamic modelling," *International Journal of Electrical Power & Energy Systems*, vol. 15, no. 5, pp. 315–321, Jan. 1993.

[90] J. G. Njiri and D. Söffker, "State-of-the-art in wind turbine control: Trends and challenges," *Renewable and Sustainable Energy Reviews*, vol. 60, pp. 377–393, 2016.

[91] A. Jafari and G. Shahgholian, "Analysis and simulation of a sliding mode controller for mechanical part of a doubly-fed induction generator based wind turbine," *IET Generation, Transmission & Distribution*, vol. 11, no. 10, pp. 2677–2688, 2017.

[92] M. Zamanifar, B. Fani, M. E. H. Golshan, and H. R. Karshenas, "Dynamic modeling and optimal control of DFIG wind energy systems using DFT and NSGA-II," *Electric Power Systems Research*, vol. 108, pp. 50–58, 2014.

[93] N. Pogaku, M. Prodanovic, and T. C. Green, "Modeling, analysis and testing of autonomous operation of an inverter-based microgrid," *IEEE Transactions on Power Electronics*, vol. 22, no. 2, pp. 613–625, 2007.

[94] J. Rocabert, A. Luna, F. Blaabjerg, and P. Rodríguez, "Control of power converters in AC microgrids," *IEEE Transactions on Power Electronics*, vol. 27, no. 11, pp. 4734–4749, 2012.

[95] S. Adhikari, F. Li, and H. Li, "P-Q and P-V control of photovoltaic generators in distribution systems," *IEEE Transactions Smart Grids*, vol. 6, no. 6, pp. 2929–2941, 2015.

[96] M. Ilić, R. Jaddivada, and X. Miao, "Modeling and analysis methods for assessing stability of microgrids," *IFAC-PapersOnLine*, vol. 50, no. 1, pp. 5448–5455, 2017.

[97] Q.-C. Zhong, "Power-electronics-enabled autonomous power systems: Architecture and technical routes," *IEEE Transactions on Industrial Electronics*, vol. 64, no. 7, pp. 5907–5918, 2017.

[98] X. Wang, L. Harnefors, and F. Blaabjerg, "A unified impedance model of grid-connected voltage-source converters," *IEEE Transactions on Power Electronics*, 2017.

[99] C. Buccella, C. Cecati, H. Latafat, and K. Razi, "Multi string grid-connected PV system with LLC resonant DC/DC converter," *Intelligent Industrial Systems*, vol. 1, no. 1, pp. 37–49, 2015.